InP-based dilute-nitride mid-infrared type-II "W" quantum-well lasers

I. Vurgaftman and J. R. Meyer
Code 5613, Naval Research Laboratory, Washington DC 20375

N. Tansu
Center for Optical Technology, Department of Electrical and Computer Engineering, Lehigh University, Bethlehem, Pennsylvania 18015

L. J. Mawst
Reed Center for Photonics, Department of Electrical and Computer Engineering, University of Wisconsin-Madison, Madison, Wisconsin 53706-1691

(Received 29 June 2004; accepted 29 July 2004)

We propose and simulate dilute-nitride midwave-infrared (3–6 μm) laser structures, whose type-II "W" active regions (InAsN/GaAsSb/InAsN/GaInP) are designed for growth on InP substrates. Besides taking advantage of the relative maturity of InP-based processing technology, this approach allows the substrate to serve as the bottom optical cladding layer, and for a top InP clad to provide high thermal conductivity for epitaxial-side-down mounting. Band structure and optical analyses project that the proposed lasers should produce nearly as much gain as current type-II W devices on GaSb substrates. © *2004 American Institute of Physics*. [DOI: 10.1063/1.1794898]

Numerous commercial and military applications will require high-performance semiconductor lasers emitting in the midwave-infrared spectral region. Although InP-based quantum-cascade lasers have recently reached room-temperature continuous-wave (cw) operation at $\lambda = 4.6–9.1$ μm,[1,2] for shorter mid-IR wavelengths (down to $\lambda = 3.04$ μm[3]) the leading III-V diode lasers[4,5] have employed type-II "W" active regions[6] grown on GaSb substrates. In the interband cascade configuration,[7,8] antimonide W lasers have operated cw to $T_{max} = 214$ K. However, their progress has been slowed by the need to overcome significant challenges associated with the immature GaSb-based growth and processing technologies.

We propose and analyze the gain properties of a new type of dilute-nitride mid-IR W diode laser that can be grown on InP. We show that this structure with InAsN electron quantum wells (QWs) retains the usual advantages of a W laser, which include strong wave function overlap to provide high gain despite the type-II band alignment. The present device, which resembles somewhat the GaAs-based dilute-N W laser that we recently proposed for emission at 1.55 μm,[9,10] would have several advantages over analogous antimonide mid-IR devices. These InP advantages include (1) a much more mature growth and fabrication technology, (2) a simplified epitaxial structure, because the InP substrate also serves as the bottom optical cladding layer, (3) improved heat dissipation, following overgrowth of an InP top clad or buried heterostructure, and (4) the option of using a high-power near-IR diode array to optically pump an epitaxial-side-down-mounted device through the transparent substrate.

Figure 1 shows the band profiles, energy levels, and selected wave functions for one period of a dilute-N W active region. The central $GaAs_{0.65}Sb_{0.35}$ hole QW of thickness 20 Å is sandwiched between two 27 Å $InAs_{0.95}N_{0.05}$ electron QWs, which are in turn surrounded by 70 Å thick $Ga_{0.25}In_{0.75}P$ barriers. The chosen GaInP thickness fixes the E1S miniband width at ≈10 meV, which should be sufficient to assure interperiod electron tunneling without substantially impacting the differential gain at 300 K. This structure is projected to emit at 3.8 μm when operated at room temperature, although wavelengths ranging from 3 μm to 6 μm should be attainable by varying the layer thicknesses. For the design in Fig. 1, the compressive strain of 2.2% in the InAsN QWs is partly offset by tensile strains of 1.1% and 0.9% in the hole QW and barrier, respectively. Although the strain is not strictly compensated here, for these thin layers and a small number of active periods the strain accumulation should not be enough to induce significant dislocation densities. As in antimonide W configurations, the large band offsets strongly confine both types of carriers.[6] We further note that this device structure is Al-free, which is (1) advantageous for realizing etched and regrown structures due to its low reactivity to O_2, and (2) less susceptible to bulk and facet degradation. Furthermore, the proposed active regions

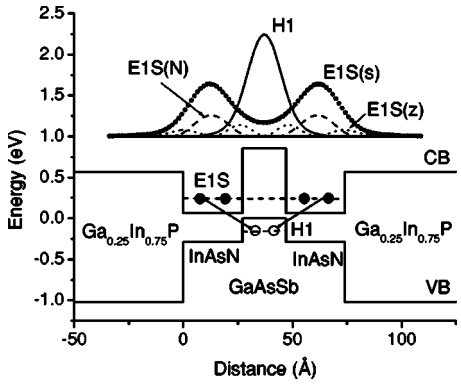

FIG. 1. Band profiles, energy levels, and selected wave function components for one period of the 27 Å $InAs_{0.95}N_{0.05}$/20 Å $GaAs_{0.65}Sb_{0.35}$/27 Å $InAs_{0.95}N_{0.05}$/70 Å $Ga_{0.25}In_{0.75}P$ mid-IR "W" active region designed for emission at 3.8 μm.

can be grown by either molecular beam epitaxy (MBE) or metalorganic chemical vapor deposition. Antimonide W structures require Al-containing barriers for good hole confinement and have only been grown by MBE.

Energy dispersion relations, wave functions, and optical matrix elements have been calculated using a ten-band $\mathbf{k}\cdot\mathbf{p}$ formalism that includes N-like and Γ-like conduction bands, as well as heavy-, light-, and split-off holes. As in our previous analysis of GaAs-based dilute-N W lasers for emission at 1.55 μm,[9] we use the band anticrossing (BAC) model[11] to account for interactions between the Γ-like and N-like states in the dilute-N layers.[12] Band parameters for the non-nitride and dilute-N materials are taken from our recent reviews.[13,14] Briefly, for InAsN we employ a coupling potential of $V=2.0$ eV and an N-level position of 1.086 eV above the InAs conduction band minimum at $T=300$ K. We assume that interaction with the N level does not affect the position of the InAsN valence band. While the unstrained valence-band offset (VBO) between GaAsSb and InAs has not been fully characterized, the resulting uncertainty affects only the details of this study rather than the main conclusions. The InAsN/InAs VBO is most likely quite small, and for definiteness is assumed to vanish.[14] In the dilute-N layer, strain effects are included into the host (nitrogen-free) conduction-band position, and interactions with the N level are then introduced as in the unstrained material. The resulting Hamiltonian is diagonalized in reciprocal space, with a wave vector cutoff of $\approx 0.2(2\pi/a)$ imposed to avoid the introduction of spurious states.

The upper portion of Fig. 1 illustrates some key electron and hole wave functions derived from these calculations. Owing to the strong coupling with nitrogen states in the InAsN layer, the E1S wave function has a significant N-like component (dashed curve). The Γ-like component is further comprised of *s*-like (curve with points) and p_z-like (due to mixing with light hole states, dotted curve) constituents. According to our calculations, ≈18% of $|\Psi_{E1S}|^2$ is N-like at the zone center (dashed curve in Fig. 1) and hence does not contribute to the optical gain. The other 82% can contribute because it is Γ-like, and also exhibits stronger overlap with the hole wave function Ψ_{H1} (solid curve). The square of the type-II optical matrix element at the zone center is ≈29% of that for bulk InAs, which is comparable to the result for antimonide W structures.[6] Because the lowest antisymmetric electron subband (E1A) is ≈100 meV higher in energy than E1S (see Fig. 2), it should not deplete any significant fraction of the injected electrons from the lasing level.

An advantage of the structure of Fig. 1 is that the *tensile* strain in the hole QW helps to balance the compressive strain in the electron QWs. However, the valence-band in-plane dispersion relations for that structure (dashed curves in Fig. 2) are far from optimal. Note that the first heavy- (H1) and light-hole (L1) subbands anticross at $\approx 0.03(2\pi/a)$, because tensile strain counteracts the confinement-induced splitting of H1 and L1. The anticrossing induces a high density of states near the band edge, which is undesirable since more holes must then be injected to achieve a population inversion. On the other hand, a smaller hole mass near the band edge increases the differential gain while also suppressing nonradiative Auger recombination.[15] We therefore consider an alternative design that features *compressive* strain in the hole QWs (also projected to emit at 3.8 μm): 12 Å $InAs_{0.97}N_{0.03}$/20 Å $GaAs_{0.35}Sb_{0.65}$/12 Å $InAs_{0.97}N_{0.03}$/130 Å $Ga_{0.25}In_{0.75}P$. While the band profiles and wave functions are qualitatively similar to those in Fig. 1, the in-plane dispersion relations in Fig. 2 (solid curves) are much more advantageous, since the enhanced H1/L1 splitting moves the anticrossing much farther out, and causes the hole mass to remain light ($\approx 0.085 m_0$) over a much wider range of energies. Although the compressive strain per period is larger for this design, the net strain accumulated within a device with relatively few periods should still be acceptable.

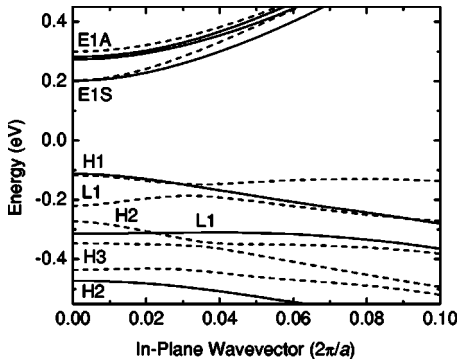

FIG. 2. Conduction and valence band in-plane dispersion relations for the *tensile* (dashed) and *compressively* strained (solid) dilute-N W laser structures.

We have derived optical gains for the two dilute-N W structures, and compared with results for a typical antimonide W structure [20 Å InAs/25 Å $Ga_{0.72}In_{0.28}Sb$/20 Å InAs/35 Å AlSb] designed to emit at the same wavelength. All three calculations assume a Gaussian broadening linewidth of 5 meV, which was recently found to be consistent with photoluminescence and lasing measurements on antimonide W devices.[16] Gain dependences on the injected carrier density at room temperature are illustrated in Fig. 3. Whereas the dilute-N structure with *tensile* strain has a considerably higher transparency carrier density and lower differential gain than the antimonide W, the *compressively* strained dilute-N structure is much more attractive. Both the

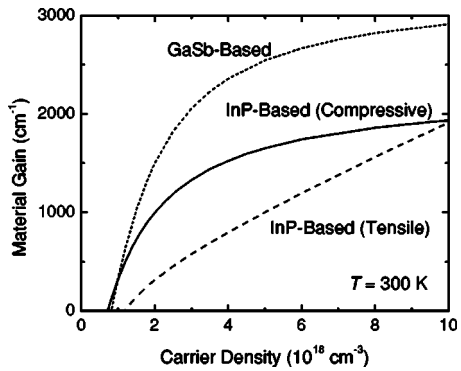

FIG. 3. Optical gain vs carrier density for the structures with tensile (dashed) and compressive (solid) strain in the hole QW, along with results for a representative antimonide W structure (dotted).

differential gain and the maximum gain are 65–67 % of those in the antimonide W material, and the transparency carrier densities are nearly identical.

If we design a full laser structure by incorporating a 0.3 μm thick $In_{0.53}Ga_{0.47}As$ separate-confinement region on each side of the active region and a 2 μm thick InP top optical cladding layer (with the InP substrate acting as the bottom clad), we calculate an optical confinement factor of 1.4% per QW. Depending on the magnitude of the internal loss, roughly five QW periods should be optimal for high-power cw operation as a room-temperature edge-emitting diode laser. Mid-IR vertical-cavity surface-emitting lasers should also be feasible using the dilute-N W active region.

The high-temperature carrier lifetimes in interband mid-IR laser materials remain somewhat controversial. While it is well established that the nonradiative Auger process dominates[17] (whereas Shockley-Read and radiative recombination were more prominent at lower T), it is less clear whether the decay is due mostly to multielectron or multihole Auger processes.[18] The former is minimized by a small hole mass near the band edge,[15] a condition that is fulfilled by the *compressively* strained dilute-N structure. While multihole Auger decay should be minimized when intervalence resonances are avoided,[19] there have been no unambiguous confirmations of a direct correlation between intervalence resonances and recombination lifetime.[17,18] The relatively thin electron and hole QW layers, along with the large VBO of the GaInP barriers, should in principle permit significant flexibility in engineering the final-state valence-band alignments.[19] Similar considerations may also apply to minimization of the internal losses[20,21] in mid-IR dilute-N W lasers, since intervalence processes in the active region can contribute substantially to the net absorption in the cavity.[22,23] Although in the near term the relatively poorer growth quality of dilute-N layers may reduce the Shockley-Read lifetimes by comparison to those in non-N-containing InP-based structures grown by more mature methods, this limitation may be overcome as the technology for dilute nitrides continues to advance.[24] Recent progress in dilute-N laser technology has resulted in a significant improvement of the lasing performance at wavelengths of interest for telecommunications[25] and concurs well with its continuing trend of advancement.

We conclude that there is no fundamental reason to expect the performance characteristics of dilute-N W lasers to be significantly inferior to those of antimonide W lasers emitting at the same wavelength. While the optical matrix elements and differential gains are incrementally lower, those considerations may be more than offset by the prospects for improved heat dissipation and exploitation of the more mature growth and processing technologies for InP-based optoelectronic devices.

The work at NRL was supported by ONR. The work at UW-Madison was supported by NSF Grant No. 0355442.

[1]M. Beck, D. Hofstetter, T. Aellen, J. Faist, U. Oesterle, M. Ilegems, E. Gini, and H. Melchior, Science **295**, 301 (2002).
[2]A. Evans, J. S. Yu, L. Doris, K. Mi, S. Slivken, and M. Razeghi, Appl. Phys. Lett. **84**, 314 (2004), shorter-wavelength data to be published.
[3]C. Lin, M. Grau, O. Dier, and M.-C. Amann, Appl. Phys. Lett. **84**, 5088 (2004).
[4]W. W. Bewley, H. Lee, I. Vurgaftman, *et al.*, Appl. Phys. Lett. **76**, 256 (2000).
[5]M. Kim, W. W. Bewley, J. R. Lindle, C. S. Kim, I. Vurgaftman, J. R. Meyer, J. G. K. Kim, and R. U. Martinelli, Appl. Phys. Lett. **83**, 5374 (2003).
[6]J. R. Meyer, C. A. Hoffman, F. J. Bartoli, and L. R. Ram-Mohan, Appl. Phys. Lett. **67**, 757 (1995).
[7]R. Q. Yang, C. J. Hill, B. Yang, and C. M. Wong, IEEE Photonics Technol. Lett. **16**, 987 (2004).
[8]J. L. Bradshaw, N. P. Breznay, J. D. Bruno, *et al.*, Photonics Spectra **20**, 479 (2004).
[9]I. Vurgaftman, J. R. Meyer, N. Tansu, and L. J. Mawst, Appl. Phys. Lett. **83**, 2742 (2003).
[10]N. Tansu and L. J. Mawst, IEEE J. Quantum Electron. **39**, 1205 (2003).
[11]J. Wu, W. Shan, and W. Walukiewicz, Semicond. Sci. Technol. **17**, 860 (2002).
[12]S. A. Choulis, T. J. C. Hosea, S. Tomic, *et al.*, Phys. Rev. B **66**, 165321 (2002).
[13]I. Vurgaftman, J. R. Meyer, and L. R. Ram-Mohan, J. Appl. Phys. **89**, 5815 (2001).
[14]I. Vurgaftman and J. R. Meyer, J. Appl. Phys. **94**, 3675 (2003).
[15]H. P. Hjalmarson and S. R. Kurtz, Appl. Phys. Lett. **69**, 949 (1996).
[16]C. L. Canedy, W. W. Bewley, C. S. Kim, M. Kim, I. Vurgaftman, and J. R. Meyer, J. Appl. Phys. **94**, 1347 (2003).
[17]J. R. Meyer, C. L. Felix, W. W. Bewley, *et al.*, Appl. Phys. Lett. **73**, 2857 (1998).
[18]C. H. Grein, M. E. Flatte, J. T. Olesberg, S. A. Anson, L. Zhang, and T. F. Boggess, J. Appl. Phys. **92**, 7311 (2002).
[19]M. E. Flatte, Opt. Express **2**, 131 (1998).
[20]W. W. Bewley, I. Vurgaftman, C. L. Felix, *et al.*, J. Appl. Phys. **83**, 2384 (1998).
[21]W. H. Lau and M. E. Flatté, Appl. Phys. Lett. **80**, 1683 (2002).
[22]W. W. Bewley, C. L. Felix, I. Vurgaftman, D. W. Stokes, J. R. Meyer, H. Lee, and R. U. Martinelli, IEEE Photonics Technol. Lett. **12**, 477 (2000).
[23]R. Kaspi, A. Ongstad, G. C. Dente, J. Chavez, M. L. Tilton, and D. Gianardi, Appl. Phys. Lett. **81**, 406 (2002).
[24]S. Kurtz, J. F. Geisz, B. M. Keyes, *et al.*, Appl. Phys. Lett. **82**, 2634 (2003).
[25]N. Tansu, N. J. Kirsch, and L. J. Mawst, Appl. Phys. Lett. **81**, 2523 (2002).